This is a peer-reviewed, accepted author manuscript of the following research article: Feng, Y. L., Chen, D. Y., Li, S. W., Xiao, Q., & Li, W. (2022). Vortex-induced vibrations of flexible cylinders predicted by wake oscillator model with random components of mean drag coefficient and lift coefficient. *Ocean Engineering*, *251*, [110960]. https://doi.org/10.1016/j.oceaneng.2022.110960

Vortex-induced vibrations of flexible cylinders predicted by wake oscillator model with random components of mean drag coefficient and lift coefficient

Y.L. Feng[a,b], D.Y. Chen[a,b], S.W. Li[a1], Q.Xiao[a,c], W. Li[d]

[a]Institute of Ocean Engineering, Shenzhen International Graduate School, Tsinghua University, Shenzhen 518055, Guangdong, China

[b]School of Environment, Tsinghua University, Beijing 100084, China

[c]Department of Naval Architecture, Ocean and Marine Engineering, University of Strathclyde, Henry Dyer Building, Glasgow G4 0LZ, Scotland, UK

[d]Key Laboratory of Far-shore Wind Power Technology of Zhejiang Province, Hangzhou, 311122, Zhejiang, China

Abstract

In the present study, vortex-induced vibrations in both In-Line and Cross-Flow directions of long flexible cylinders within a uniform flow are predicted by a modified wake oscillator model. In detail, the Van der Pol's wake oscillator model with the drag and lift coefficients being modelled as random variables. The statistics of the force coefficient, i.e. mean value and standard deviation, are extracted from the literature reporting experimental measurements and numerical simulation results of the drag and lift forces experienced by the cylinder-type structure. With the statistics, a series of pseudo stochastic variables are generated to calculate the drag and lift forces. In Euler-Bernoulli equation governing the motion of the cylinder, tension is modelled as a function of flow velocity. Through comparing the predictions from the model with and without randomness to the experimental results, it is found that the scatter in vibration amplitudes, multi-frequency effect (broadband stochastic process) and frequency multiplication effect are successfully reproduced by the model with randomly drawn drag and lift coefficients. However, the overestimate of the oscillation frequency for the In-Line vibrations implies that the In-Line coupling is still a topic that deserves a further investigation.

Key words: Vortex-induced vibration; Wake oscillator model; Pseudo Stochastic Variables; Combined inline-cross flow responses

Introduction

[1] Corresponding Author: Sunwei, Li, li.sunwei@sz.tsinghua.edu.cn

Given more ambient resources and less environmental impacts, offshore oil/gas exploration has shifted from shallow waters to the deep sea. For exploring the oil and gas resources in the deep sea, facilities currently employed in the offshore industry should be modified. Particularly, working risers in the deep sea are even more slender in comparing with the risers in relatively shallow waters. For the slender structures erected in the ocean, the structural flexibility is certainly coupled with the flow influencing the Vortex-induced vibrations (VIV) of the structure. Consequently, the VIV of risers are of practical interest in ocean engineering.

Very few in-situ observations of VIV of ocean engineering structures and other full-scale slender bodies are reported in the literature in contrast to numerous results from scaled-down experiments, computational fluid dynamics (CFD) simulations and empirical models. During the past decades, characteristics of the VIV occurred for the long flexible cylinder with high aspect ratios have been studied and reported, such as high harmonics, high mode numbers, multi-mode (multi-frequency) responses (Baarholm et al., 2006; Bourdier and Chaplin, 2012; Chaplin et al., 2005; Gopalkrishnan, 1993; Khalak and Williamson, 1999; Lie and Kaasen, 2006; Liu et al., 2014) and traveling waves (Song et al., 2011). In reality, VIV observed in wave-basin experiments and in field measurements acquires two features shared with other fluid-structure interaction problems (Cavalcante et al., 2007). The first feature relates to the scatter or the discrepancy of the measurements, which reflects that the experiments yield, regardless of the identical model and environmental conditions, slightly different results due to the random nature of VIV-related phenomenon. The second feature is that the VIV observed in experiments often contains multiple frequencies. The reason for observations of multiple frequencies is probably the random disturbance coming from the stochastic flow variation, the structural imperfections, measurement errors, chaotic nature of the vortex-shedding and instinct nonlinear characteristics of VIV. However, most empirical and CFD model analyze VIV in a deterministic way and discern the vibration with clearly defined amplitudes, frequencies and modes. The deterministic approach ignores the ubiquitous random effects which is natural and important.

Given the stochastic nature of VIV, and hence the scatter of measurements taken in the experiments, previous studies have been carried out to assess the uncertainties and randomness in the VIV. Pioneered in the field, Billah and Shinozuka (1991) solved the single degree-of-freedom (DOF) equation for flow-induced vibration theoretically when the flow velocity exciting the vibration is taken as a random variable of either a white noises or Gaussians type. In fact, the flow velocity is decomposed in their study into a constant mean, and a random fluctuation. Their investigation concluded that the random fluctuation in the deterministic equations have to be treated as the colored noise because of the non-linear control parameter. Lucor and Karniadakis (2004) reviewed direct numerical simulations of flow-structure interactions in both deterministic and stochastic ways and solved the coupled stochastic Navier-Stokes and structure motion equations via Wiener-Askey Polynomials Chaos method for the VIV. In their two-dimensional rigid cylinder model, the structural properties, i.e. the damping coefficient and structural stiffness, and boundary conditions are taken as random processes. For example, the damping coefficient in their study is modelled as the sum of the mean value and a random disturbance, which is related to the standard deviation of the damping coefficient. Using their model, it is feasible to efficiently assess the uncertainties associated with the flow-structure interactions. Pan et al. (2007) studied the VIV of an elastically mounted rigid cylinder at low mass-damping ratio through solving the Reynolds-Averaged Navier-Stokes (RANS) equation coupled with k-ω Shear-Stress Transport (SST) turbulence model, which induces random-type fluctuations in the prediction of the VIV. Comparing to other experimental and numerical results, their results were found statistically stable because the RANS simulation erased the randomness induced by turbulences. These comparisons between RANS results and the experimental data with the randomness reveal the VIV's random characteristics and the effect of the random disturbance on the experimental observation. Zong and Feng (2017), following the trend, developed a pseudo-stochastic method to analyze the VIV of single DOF and two DOFs systems, replacing the Monte-Carlo simulation of high computational costs. As for the wake oscillator model predicting the VIV, there have only been a few studies paid attentions to the stochastic characteristics. Srinil et al. (2018), as one of the studies, attributed the discrepancy of the measured maximum

vibration amplitude to the variations in values of empirical parameters and conducted a series of sensitive analysis on the parameters in empirical models to predict both In-Line (IL) and Cross-Flow (CF) vibrations. Shoshani (2018), in addition, investigated the theoretical solution of the lock-in phenomenon for rigid cylinder in both deterministic and stochastic ways, and Mukundan et al. (2009) improved the Van der Pol type wake oscillator model through adding random parameters, such as drag and lift coefficients, which yields better agreements with the experimental results. Imaoka et al. (2014, 2015) also discussed the inclusion of random components for modelling external forces and vortex shedding frequencies in their single DOF model.

As the review of previous studies shows, the studies on modelling the stochastic nature of VIV are, for one thing, rare. Especially for the widely used wake oscillator model, the stochastic characteristics of the VIV is entirely ignored in its prediction. The existing investigations concerning the stochastic characteristics of VIV, on the other hand, mainly targeted the rigid body. Consequently, the more realistic case where the long flexible cylinder is randomly excited by the external flow is seldom studied via empirical/engineering models. For example, the wake oscillator model, which has already been widely applied in the assessment of VIV influences on the safety of riser-type structures, has yet been employed in an investigation of stochastic and complex flow-structure interaction found in reality. Since the coupling with randomness between a riser-type structure and flow where the Euler-Bernoulli beam assumption is implied is fundamentally different from the coupling without randomness concerning 1-DOF or 2-DOF systems, it is worthwhile to systematically investigate the influence of pseudo-stochastic parameterization in the wake oscillator model in predicting the VIV of long flexible cylinders.

Given the lack of model studies considering the stochastic characteristics of VIV, the present study includes a pseudo-random variable generation scheme to provide more realistically drag and lift coefficients in the wake oscillator model. In fact, the present study is motivated by the need to explain the discrepancies between experimental results and model predictions of VIV of a long flexible cylinder. In the wake oscillator model under investigation, the drag and lift coefficients are pseudo-random variables whose statistics agreeing with experimental and numerical simulation results reported in the literature. Compared to previous studies concerning the VIV, the present work has several advantages as: 1) a three-dimensional model for long flexible cylinders is presented to predict both CF and IL vibrations; 2) the schemes to generate pseudo-random variables representing drag and lift coefficients; 3) a coupling scheme between the stochastic wake oscillator model and long flexible structural model presenting more realistic predictions of the VIV.

After this introduction, section 2 presents the improved model including structural motion equation, wake oscillator model and the schemes to generate pseudo-random variables with statistics agreeing to the scattered drag and lift coefficients measured in previous studies. In section 3, the predictions made by this innovative model considering stochastic drag and lift coefficients are compared with the experimental results and model predictions reported in literatures. The influence of stochastic drag and lift coefficients on the model predictions are therefore discussed based on the comparisons. Conclusion remarks are presented in section 4.

2. Model description

2.1 Wake oscillator model

The marine riser is often simplified as a flexible cylinder described by Euler-Bernoulli beam equation (Gu et al., 2012; Hong and Shah, 2018). The riser's motions are therefore modelled as the deformation of the beam. In the present study, the Euler-Bernoulli beam equation is used to simulate the VIV experienced by a riser. In detail, the solution to the equation yields the displacements in x and y axes of the cylinder at a given z coordinate. While the vibrations in the x and y axes are usually termed as In-Line (IL) and Cross-Flow (CF) VIV, the z axis defined along the riser when it is at the rest. In fact, the x and y

displacements of the cylinder can be expressed as,

$$M\frac{\partial^2 r}{\partial t^2}+R\frac{\partial r}{\partial t}+\frac{\partial^2}{\partial z^2}\left(EI\frac{\partial^2 r}{\partial z^2}\right)-\frac{\partial}{\partial z}\left(T\frac{\partial r}{\partial z}\right)=F \tag{1}$$

In equation (1), the symbols are defined as,

$$r=x+\mathrm{i}y,\ F=F_x+iF_y,\ M=m_s+\frac{\pi}{4}C_a\rho D^2,\ R=R_s+R_f=2\xi_d M\Omega_s+\gamma\rho D^2\Omega_f,\ \Omega_s=\sqrt{\frac{\Omega_n^2}{1+\frac{C_a}{\frac{m_s}{\frac{\pi}{4}\rho D^2}}}}. \tag{2}$$

It is noted that the meanings of the symbols used here and in the following text are consistent with the derivation presented by Feng et al. (2019), which are also listed in APPENDIX: LIST of SYMBOLS. For more details about the model derivations and limitations, readers are suggested to refer to the work of Feng et al. (2019). In equations (1-2), the displacement vector of *r* and the excitation force vector of *F* are represented by complexes and *i* is the imaginary unit. The total mass *M* is the sum of the structural mass m_s in the air and added mass. The total damping *R* includes structural damping R_s and fluid damping R_f. The natural frequencies of the cylinder in water are calculated based on the natural frequencies in the air when the effect of added masses are taken into consideration.

It should be noted that, the tension is included in the model via the term $(\frac{\partial}{\partial \mathrm{z}}(T\frac{\partial \mathrm{y}}{\partial \mathrm{z}}))$, which theoretically alters the stiffness of the riser significantly and therefore modifies the motion of the riser. In equation (1), the tension is actually considered as a function of the vertical coordinate of z, which unavoidably induces extra computational burden in numerically seeking its solution as discussed in Feng et al. (2019). Therefore, the tension is assumed constant along the length of the cylinder as in the previous studies (Gu et al., 2012; Gu et al., 2013). The beam deformation, axial tension (Gu et al., 2013) and the vibration frequency (Lee and Allen, 2010) of a riser are found, however, increase with the free stream velocity. Therefore, it is suggested, following Feng et al. (2019), that the tension should be modelled as a constant along the axis of the riser but varies with the external free stream velocity as,

$$T=T_{ini}+\frac{EA}{16\pi^2}\left(\frac{\rho DU^2C_{D0}L^3}{EI\pi^2+TL^2}\right)^2. \tag{3}$$

For the meanings of symbols in equation (3) and equations in the rest of the manuscript, the APPENDIX: LIST of SYMBOLS should be referenced.

The external force in the x direction, i.e. IL direction, is the drag force F_x, which is modelled as the summation of the mean part f_D and the stochastically fluctuating part f'_D in the present study as

$$F_x=f_D+f_D'. \tag{4}$$

From the conventional formulation of the wake oscillator model, the mean and stochastically fluctuating parts of the drag could be modelled as,

$$f_D=\frac{1}{2}C_D\rho DU^2=\frac{1}{2}C_{D0}(1+Kq^2)\rho DU^2, \tag{5}$$

$$f_D'=\frac{1}{2}C_{Di}\rho DU^2. \tag{6}$$

In addition, the lift force driving the cylinder to move in the CF direction is calculated according to the wake oscillator model

as,

$$F_y = \frac{1}{2} C_L \rho D U^2. \quad (7)$$

In the models, the drag and lift coefficients are the essential components of the model, and are calculated as,

$$C_{Di} = C_{Di0} \frac{p}{2}, \; C_L = C_{L0} \frac{q}{2}. \quad (8)$$

In equations (5-8), C_D and C_{D0} are the mean drag coefficient and its amplitude of a stationary rigid cylinder, respectively, C_{Di} and C_L are the vortex-shedding drag and lift coefficients, C_{Di0} is the amplitude of vortex shedding drag coefficient and C_{L0} is the lift coefficient of a stationary rigid cylinder. Compared to the amplitude of the mean drag coefficient C_{D0}, C_{Di0}, determined by the vortex-shedding mechanism, is smaller by an order of magnitude, and has less experimental measurements or numerical results in the range of the Reynolds number of interest. Thus, the randomness of C_{Di} is ignored in the present study. The stochastic characteristics of C_{D0} and C_{L0} are, however, systematically involved in the model described in the present study.

In the conventional wake oscillator model, the drag and lift forces attributed to the vortex-shedding are modelled by the Van der Pol nonlinear equations. The Van der Pol equations read,

$$\frac{\partial^2 p}{\partial t^2} + 2\varepsilon_x \Omega_f (p^2 - 1) \frac{\partial p}{\partial t} + 4\Omega_f^2 p = \frac{A_x}{D} \frac{\partial^2 x}{\partial t^2}, \quad (9)$$

$$\frac{\partial^2 q}{\partial t^2} + 2\varepsilon_y \Omega_f (q^2 - 1) \frac{\partial q}{\partial t} + 4\Omega_f^2 q = \frac{A_y}{D} \frac{\partial^2 y}{\partial t^2}, \quad (10)$$

and, $\Omega_f = 2\pi S_t \frac{U}{D}$. (11)

In equations (9-11), ε_x, ε_y, A_x and A_y are the empirical parameters estimated from fitting the experimental measurements to the model, and Ω_f is the vortex-shedding frequency. It is noted that equation (1) describing the deformation of the cylinder is coupled with the wake oscillator model of equations (9-11) to predict the VIV. As regards the coupling scheme, it is suggested by Facchinetti et al. (2004) that the acceleration coupling would be more appropriate for the prediction of the VIV. Such a suggestion is adopted in the present study. Based on the acceleration coupling scheme, the hydrodynamic forces in the x and y directions acting on the cylinder can be expressed as,

$$F_x = f_D + f_D' - f_L \frac{\dot{y}}{U} = \frac{1}{2} C_{D0} (1 + Kq^2) \rho D U^2 + \frac{1}{2} C_{Di} \rho D U^2 - \frac{1}{2} C_{L0} \frac{q}{2} \rho D U \dot{y}, \quad (12)$$

$$F_y = f_L + f_D' \frac{\dot{y}}{U} = \frac{1}{2} C_{L0} \frac{q}{2} \rho D U^2 + \frac{1}{2} C_{Di0} \frac{p}{2} \rho D U \dot{y}. \quad (13)$$

2.2 Random component of force coefficient

It is well established that the VIV of a riser is a stochastic process in nature. The origins of this randomness include stochastic turbulences in flow, structural imperfections and surface roughness randomly distributed along the length of the riser and the nonlinearity of fluid-structure interactions, etc. It is also well established that it is difficult, if not impossible, to formulate the randomness of each factor individually. Considering that one of the most significant influences of various stochastic factors is the stochastic fluctuations in the measurements of drag and lift coefficients, the present study investigates the randomness of

VIV via stochastically modeling drag and lift coefficients. In fact, the measurements of C_{D0} and C_{L0} reported by previous studies based on either simulations or experimental observations are employed to calculate the statistics of them. Once the pseudo stochastic variables are generated with statistics based on the measurements, common models, such as the wake oscillator model, can be employed to reveal the impacts of the randomness on the VIV.

In fact, the present study assumes that the force coefficient is the summation of a constant mean and a pseudo-stochastically fluctuating part, as,

$$C_{D0} = \overline{C_{D0}} + \delta_{C_{D0}},\ C_{L0} = \overline{C_{L0}} + \delta_{C_{L0}}. \tag{14}$$

Given the stochastic nature of drag and lift coefficients, their statistics are more important in a model than the actual value used in a single simulation run. In order to provide reliable statistics of C_{D0} and C_{L0}, substantial data from experiments and numerical simulations are collected and plotted as a function of the logarithmic Reynolds number (Re) (Figure 1-2). Fitting the experimentally measured or numerical simulated mean drag coefficients with a 7th degree polynomial function yields,

$$C_{D0}\big(lg(Re)\big) = -0.0003356\big(lg(Re)\big)^8 + 0.008364\big(lg(Re)\big)^7 - 0.08037\big(lg(Re)\big)^6 + 0.3548\big(lg(Re)\big)^5 -$$

$$0.5001\big(lg(Re)\big)^4 - 1.737\big(lg(Re)\big)^3 + 8.788\big(lg(Re)\big)^2 - 15.05\big(lg(Re)\big) + 11.01. \tag{15}$$

It is shown in the figure that scatter in mean drag coefficients appears in the critical flow regime (Figure 1) and variations in the flow pattern certainly connects with *Re* based on the accumulated observations. Consequently, statistics of the stochastic drag coefficients are calculated corresponding to different *Re* ranges. It is noted that a variety of classifications, based on the *Re*, concerning the flow patterns around a circular cylinder is available from literature (Achenbach and Heinecke, 1981; Beaudan and Moin, 1994; Canuto and Taira, 2015; Derakhshandeh and Alam, 2019). In the present study, a fine classification scheme is adopted following the suggestion of Zdravkovich (1997) (Table 1). Within each *Re* regime, the statistics, mainly the mean and standard deviation, of the mean drag coefficients are calculated from experiments/numerical simulations from previous studies and presented in Table1.

As for the lift coefficient, the data shows no clear dependency on the *Re* (Figure 2). Therefore, the entire dataset containing the measurements of lift coefficients is used to estimate its mean and standard deviation, which are 0.4121 and 0.2967 respectively in the present work.

The studies from which the measurements of C_{D0} and C_{L0} are extracted are listed in Table 2. It is worthwhile to point out that the studies date back to 1959, and the total number reaches 83. Moreover, the scatter of the mean drag coefficient and lift coefficient comes from not only the randomness of the flow but also the aspect ratio (L/D), blockage and roughness of the cylinder(Achenbach and Heinecke, 1981; Farell and Blessmann, 1983; Güven et al., 1980)). It is, however, noted that both the influences of aspect ratio and surface roughness are intended to be inlcuded into the randomly varying drag and lift coefficients in the present study. Given the use of drag and lift coefficients in the wake oscillator model assumes the aspect ratio has no impacts on the determination of the hydrodynamic coefficient and the surface roughness is difficult to included in the wake oscillator model, such the inclusion of their influences in the random varying drag and lift coefficient is reasonable.

Table 1 Classification of flow patterns

Flow regime	Description	Re	$\overline{C_{D0}}$	$\delta_{C_{D0}}$

Laminar state of flow, L	L1: 'creeping' flow or non-separation regime	$0<Re<5$	9.3124	3.7681
	L2: steady separation or closed near-wake regime	$5<Re<40$	2.1352	0.6293
	L3: periodic laminar regime	$40<Re<200$	1.3534	0.1312
Transition-in-wake state of flow, TrW	TrW1: transition of laminar eddies in the wake form	$200<Re<250$	1.2732	0.0603
	TrW2: transition of an irregular eddy during its formation	$250<Re<400$	1.3291	0.2075
Transition-in-shear-layer, TrSL	TrSL1: development of transition waves	$400<Re<1\times10^3$	1.3223	0.2024
	TrSL2: formation of transition eddies	$1\times10^3<Re<2\times10^4$	1.2577	0.2785
	TrSL3: burst to turbulence	$2\times10^4<Re<1.4\times10^5$	1.0878	0.2758
Transition-in-boundary-layers, TrBL	TrBL0: precritical regime	$1.4\times10^5<Re<3\times10^5$	0.9181	0.2086
	TrBL1: one-bubble regime	$3\times10^5<Re<4\times10^5$	0.5200	0.1946
	TrBL2: two-bubble regime	$4\times10^5<Re<1\times10^6$	0.4810	0.2845
	TrBL3: supercritical regime	$1\times10^6<Re<3.5\times10^6$	0.6554	0.2631
	TrBL4: post-critical regime	$3.5\times10^6<Re<1\times10^7$	0.7373	0.1977
Fully turbulent state of flow, T		$1\times10^7<Re<\infty$	0.8555	0.0000

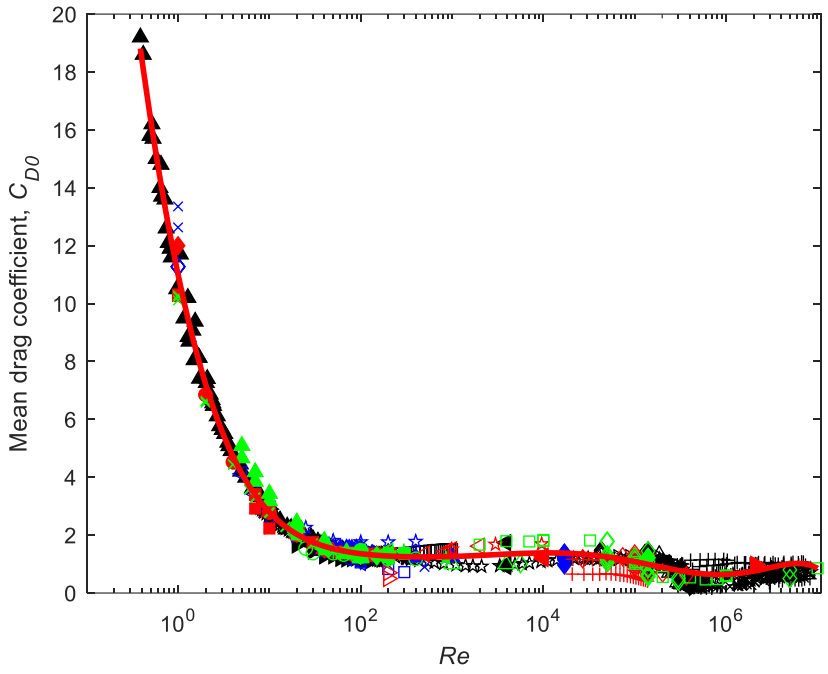

Figure 1 Collected experimental and numerical data for mean drag coefficient of flow around stationary cylinders. Data sources are listed in Table 2.

Table 2 Bibliographical of measured and computed mean drag and lift coefficients for circular cylinders

Author (Year)	C_{D0}	C_{L0}	Remarks
Achenbach and Heinecke (1981)	*		
Allen and Henning (2001)	△		
Bearman (1969)	▽	*	
Cantwell and Coles (1983)	▷		
Farell and Blessmann (1983)	◁		
Güven et al. (1980)	○		
Henderson (1995)	□		Experimental measurement
Roshko (1961)	☆		
Schewe (1983)	×	△	

Shih et al. (1993)	+		
Szepessy and Bearman (1992)	◊	▽	
Tritton (1959)	▲		
Gresho et al. (1984)		▷	
Zdravkovich (1997)		◁	
Blackburn and Melbourne (1996)		○	
Leehey and Hanson (1971)		□	
West and Apelt (1993)		☆	
Gartshore (1984)		×	
Norberg (1993)		+	
Agbaglah and Mavriplis (2019)	▼		
Baranyi and Lewis (2006)	▶	◊	
Beaudan and Moin (1994)	◀		
Belov et al. (1995)	■	▲	
Braza et al. (1985)	★	▼	
Braza et al. (1986)	●		
Breuer (2000)	◆		
Calhoun (2002)	*	▶	
Canuto and Taira (2015)	△	◀	Numerical computation
Chen et al. (2019)	▽	■	
Choi et al. (2007)	▷	★	

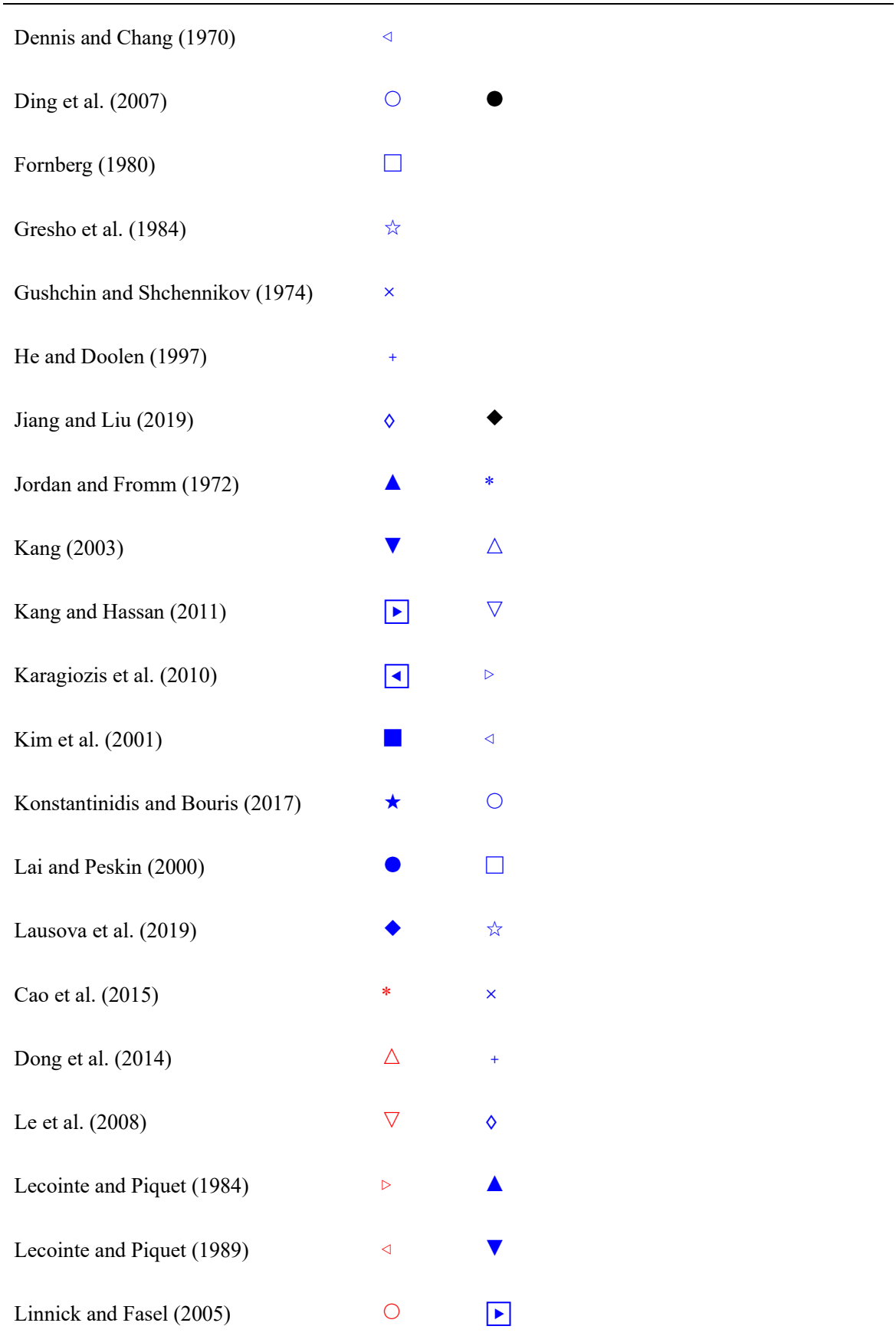
Dennis and Chang (1970)
Ding et al. (2007)
Fornberg (1980)
Gresho et al. (1984)
Gushchin and Shchennikov (1974)
He and Doolen (1997)
Jiang and Liu (2019)
Jordan and Fromm (1972)
Kang (2003)
Kang and Hassan (2011)
Karagiozis et al. (2010)
Kim et al. (2001)
Konstantinidis and Bouris (2017)
Lai and Peskin (2000)
Lausova et al. (2019)
Cao et al. (2015)
Dong et al. (2014)
Le et al. (2008)
Lecointe and Piquet (1984)
Lecointe and Piquet (1989)
Linnick and Fasel (2005)

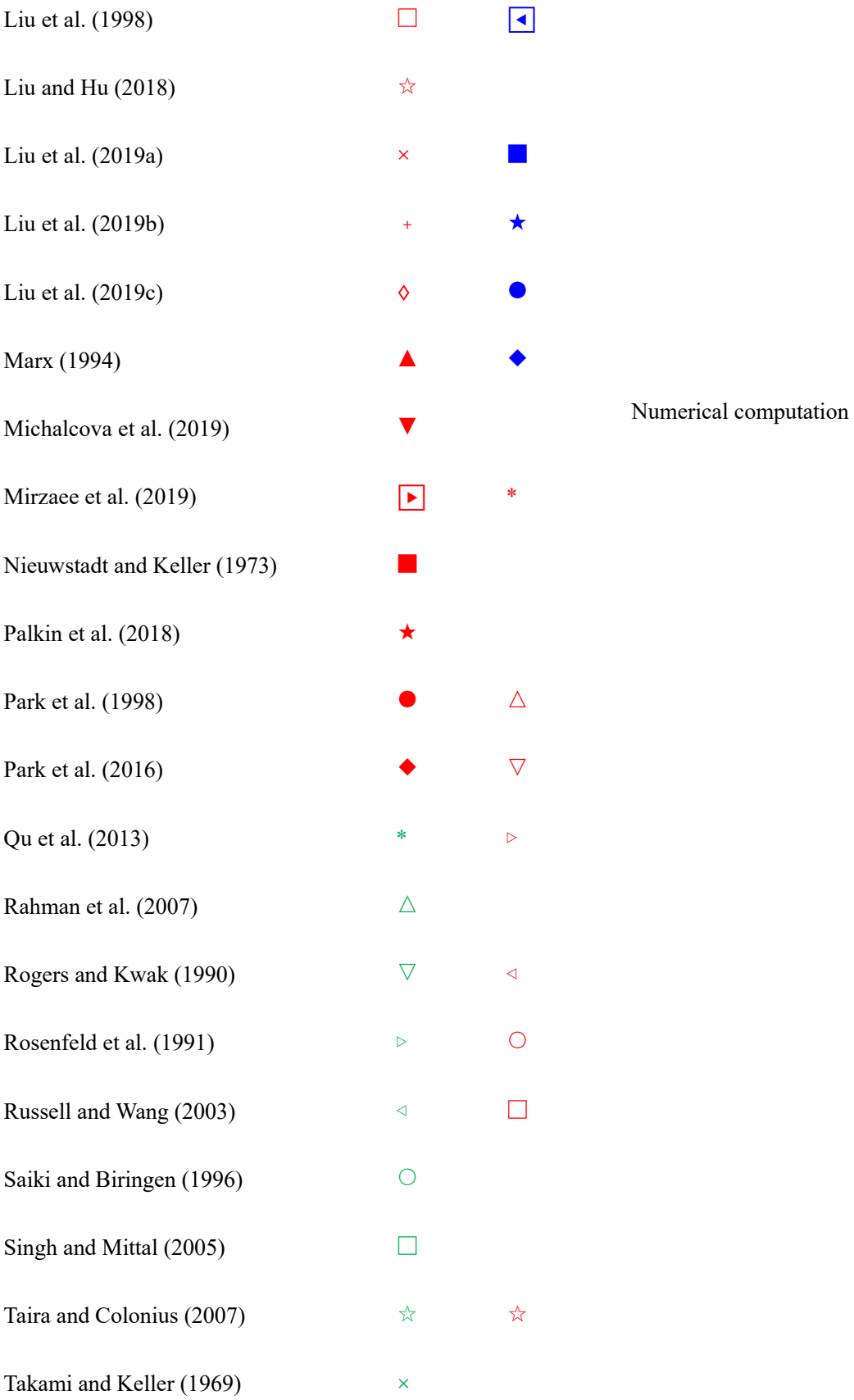
Liu et al. (1998)
Liu and Hu (2018)
Liu et al. (2019a)
Liu et al. (2019b)
Liu et al. (2019c)
Marx (1994)
Michalcova et al. (2019)
Mirzaee et al. (2019)
Nieuwstadt and Keller (1973)
Palkin et al. (2018)
Park et al. (1998)
Park et al. (2016)
Qu et al. (2013)
Rahman et al. (2007)
Rogers and Kwak (1990)
Rosenfeld et al. (1991)
Russell and Wang (2003)
Saiki and Biringen (1996)
Singh and Mittal (2005)
Taira and Colonius (2007)
Takami and Keller (1969)
Numerical computation

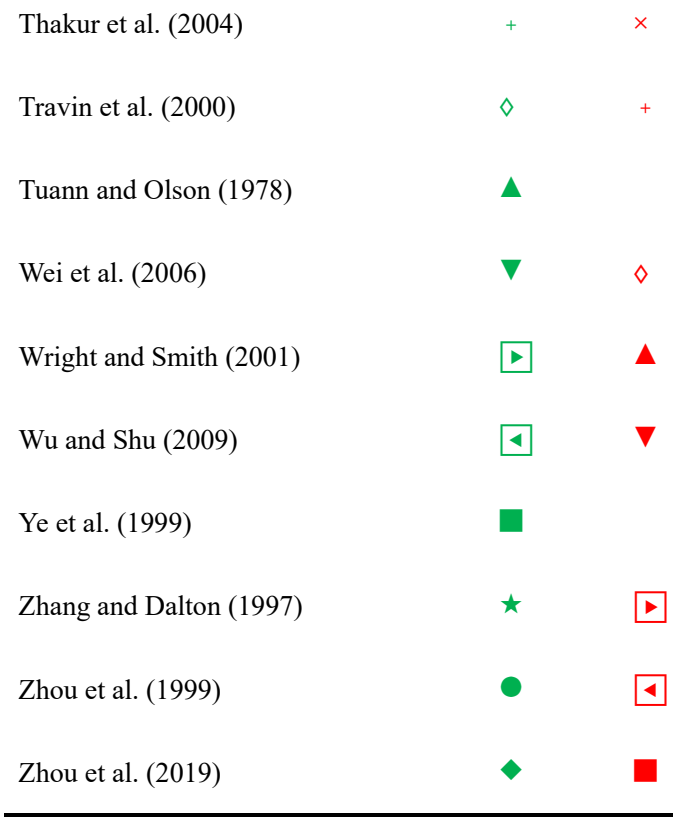

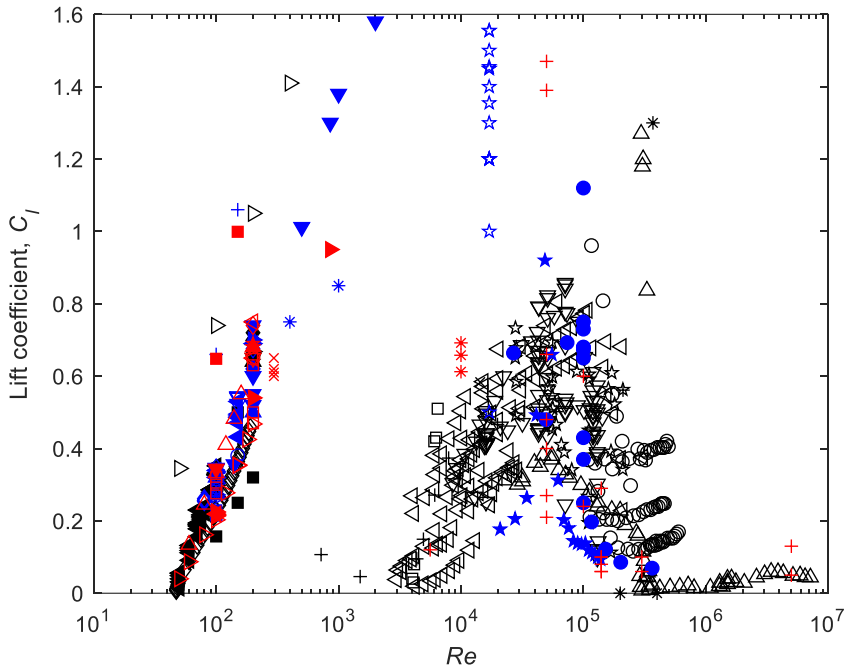

Figure 2 Collected experimental and numerical data for lift coefficient of flow around stationary cylinders. Data sources are listed in Table 2.

2.3 Boundary and initial conditions

In the prediction, the boundaries of the idealized cylinder are set to ensure the displacements and moments at both ends are zero

during the simulation. In other words, it is assumed that hinges are placed at the ends of the cylinder. The boundary conditions of the model are expressed as

$$r(0,t) = r(L,t) = 0 \qquad (t > 0) \qquad (16)$$

$$\frac{\partial^2 r}{\partial z^2}(0,t) = \frac{\partial^2 r}{\partial z^2}(L,t) = 0 \qquad (t > 0) \qquad (17)$$

The initial conditions of the model, on the other hand, are given as

$$r(z,0) = 0 \qquad \frac{\partial r}{\partial t}(z,0) = 0 \qquad (0 < z < L) \qquad (18)$$

$$p(z,0) = q(z,0) = 2 \qquad \frac{\partial p}{\partial t}(z,0) = \frac{\partial q}{\partial t}(z,0) = 0 \qquad (0 < z < L) \qquad (19)$$

Given the motion governing equations and the boundary conditions, the system is solvable to show the VIV of the idealized cylinder in a uniform flow.

2.4 Overview of the model

The model discussed in the present study is summarized in this subsection. The physical system modelling flexible riser undergoing VIV is depicted in Figure 3. The prediction of the vibrations is made through solving the structural motion equation (Equations 1, 12-13) and the Van der Pol wake oscillator equation (Equation 9-10) under the boundary condition (Equations 16-17) and initial condition (Equations 18-19). In the formula calculating the hydrodynamic forces, drag coefficient and lift coefficient are the pseudo-stochastic variables calculated according to equation (14). Their mean and standard derivation are obtained from data reported in literatures listed in Table 2. In fact, the fluctuating part of the drag and lift coefficients are generated, based on the normal probability distribution, by the MATLAB's *normrnd* function at every time step and every discrete point. It is noted that, although the Strouhal number also should be considered as a random variable in the predictions of VIV, the direct inclusion of randomly varying Strouhal numbers as the way dealing with the drag and lift coefficient in the present study leads to erroneous predictions of the dominant frequency of the VIV. Given that the randomness of Strouhal numbers influences the hydrodynamics of the cylinder in a different way, its inclusion in the developed model is our future endeavor and hence is neglected in the present study.

Considering that the system is governed by a set of partial differential equations, the central finite difference scheme is employed to solve for the time histories of vibrations or beam deformations at 201 discrete points along the cylinder with a time step of 10^{-4}. It is noted that the length of the cylinder is 38m as in the experimental study of Trim et al. (2005), and the simulation time for a single run is 80s.

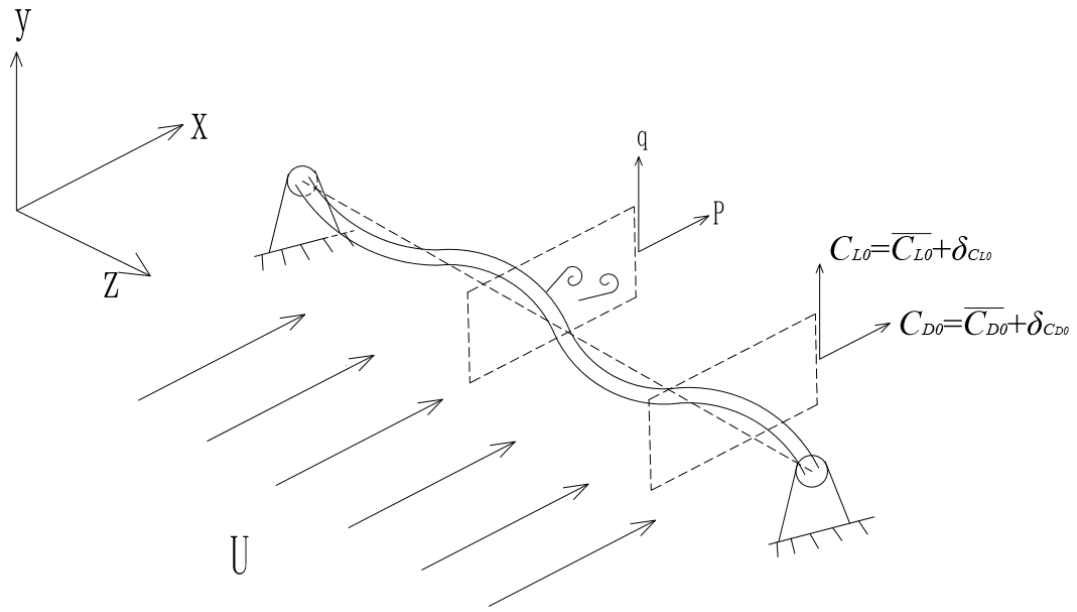

Figure 3 A schematic view of a flexible cylinder undergoing VIV in uniform flow with random effect

3. Case study

With the help of the wake oscillator with random drag and lift coefficients, the experiment conducted by Trim et al. (2005) is numerically reproduced to exhibit the influences of random hydrodynamics on the prediction of the VIV. In addition to directly comparing to the experimental data, the model predictions are also compared to the corresponding results produced by a model without random effects (Feng et al., 2019). The properties of the idealized cylinder and the values of model parameters are listed in Table 3 and 4, respectively, as reported by Feng et al. (2019). The velocities of the uniform flow ranges from 0.3m/s to 2.4m/s with an increment of 0.1m/s, which is consistent with the experiment.

Table 3 Properties of the cylinder (Trim et al., 2005)

Outer diameter	D=0.027m	Young's modulus of elasticity	E=36.2×10^{9}N/m^2
Inner diameter	d=0.021m	Axial tension	T_{ini}=4-6kN
Wall thickness	t_w=0.003m	Aspect ratio	1407
Length	L=38m	Mass ratio	1.6
Structure mass	m_s=0.939kg/m	Density	ρ=1025kg/m^3

Table 4 Values of the model parameters

Ca	1	St	0.17

C_{D0}	1.2	C_{Di0}	0.1
C_{L0}	0.3	Γ	0.45
ε_x	0.3	ε_y	0.3
A_x	12	A_y	12

Before the model predictions are utilized to discuss the influences of randomness, a number-of-runs independence check should be in place. In fact, the simulations are repeated for 50, 100 and 150 times, with randomly drawn drag and lift coefficients, at the flow velocity of 1m/s. The means and standard deviations of non-dimensional amplitude, dominant frequency and dominant mode number of the cylinder in x and y directions are extracted from the simulations and compared in Table 5. It is revealed, from the table, that the model predictions are nearly identical, which substantiates that the predictions corresponding to 100 simulation runs are sufficient for discerning the statistics of the VIV under the influence of random drag and lift coefficients.

Table 5 Mean value and standard deviation of results at U=1m/s

	Number of runs	x (IL) direction			y (CF) direction		
		Amplitude /Diameter	Frequency (Hz)	Mode No.	Amplitude /Diameter	Frequency (Hz)	Mode No.
Mean value	50	0.1660	12.5997	13	0.7874	6.1999	7
	100	0.1661	12.5997	13	0.7874	6.1999	7
	150	0.1659	12.5997	13	0.7874	6.1999	7
Standard deviation	50	0.0015	0.0000	0	0.0003	0.0000	0
	100	0.0015	0.0000	0	0.0003	0.0000	0
	150	0.0014	0.0000	0	0.0003	0.0000	0

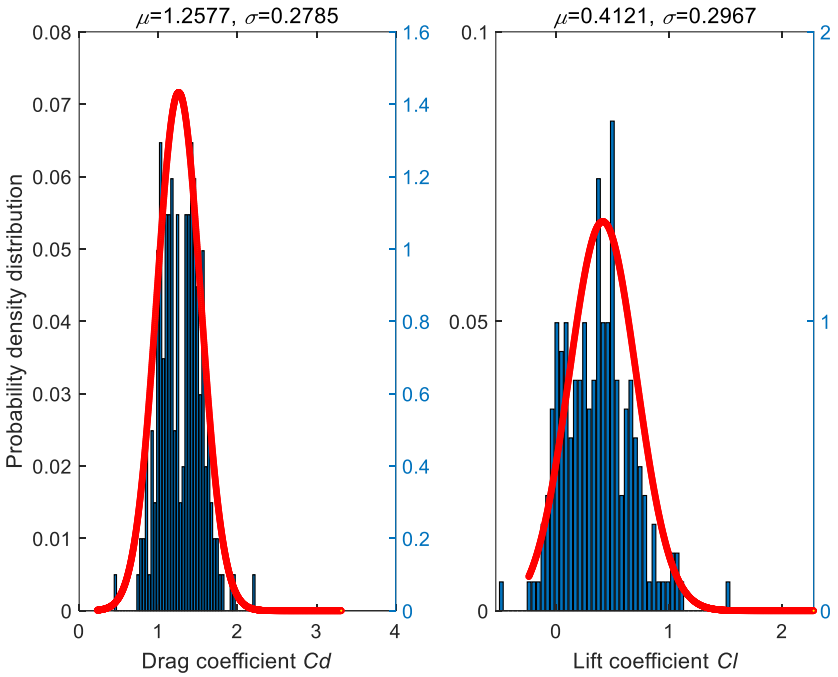

Figure 4 Probability density distribution of the drag and lift coefficient (*Re*=35100)

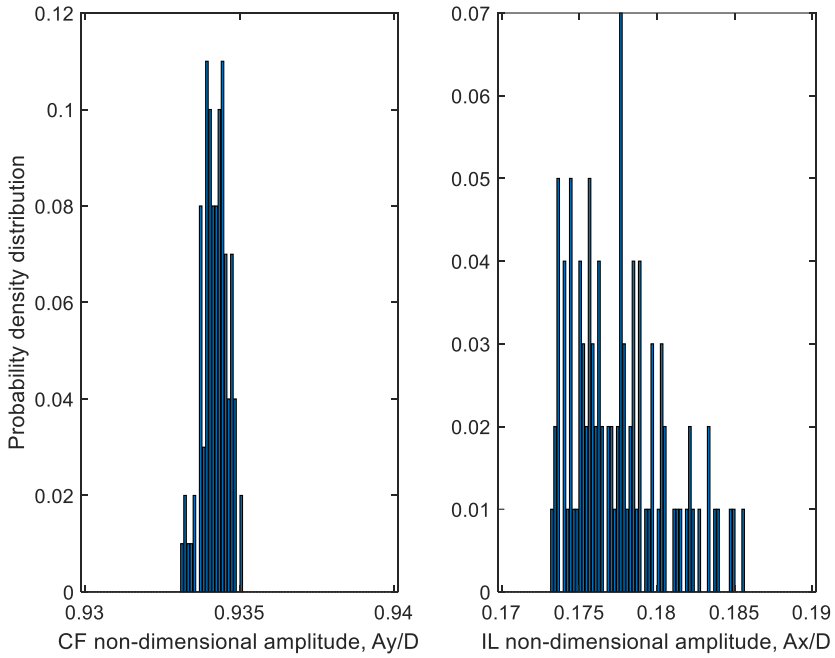

Figure 5 Probability density distribution of the non-dimensional amplitude in CF and IL directions (*Re*=35100)

Figure 4 and Figure 5 show the probability density distributions of the drag and lift coefficient and the corresponding non-dimensional vibration amplitudes in both CF and IL directions extracted from the 100 simulation runs when the flow velocity is 1.3m/s (*Re*=35100). The averaged non-dimensional vibration amplitude ξ corresponding to a single simulation run, calculated according to equation (20), is a measurement of the VIV magnitude for the entire cylinder.

$$\xi = \text{mean}(S_i), S_i = \frac{std(r_i(t))}{D} = \frac{1}{D}\sqrt{\frac{\sum_{t=t1}^{Nt}\left(r_i^{(t)} - \overline{r_i}\right)^2}{N_t - 1}} \qquad (1 \le i \le N) \qquad (20)$$

in which $\overline{r_i} = mean\left(r_i^{(t)}\right),\ t_1 \le t \le N_t$.

In equation (20), N is the node number, taking the value of 201 for the entire length of the cylinder, t_1 is the moment at which the simulation is stable, N_t is the number of time steps, S_i is the standard deviation of displacements at the node i, $r_i^{(t)}$ and $\overline{r_i}$ are the instantaneous and mean displacement at the i^{th} node, respectively. It is noted that the predictions of VIV in IL and CF directions corresponding to the model with random drag and lift coefficients are statistically agreeing with the predictions from conventional wake oscillator model. In fact, the averaged ξ corresponding to the vibrations in the CF and IL directions shown in Figure 5 are 0.934 and 0.178, respectively, comparing to the corresponding predictions of 0.584 and 0.155 from the conventional model. While the averaged ξ reveals the magnitude of vibrations, the standard deviations of ξ implies the scatter of model prediction, which in turn reflects the randomness of the model. Figure 5 indicates that the standard deviations of ξ corresponding to CF and IL vibrations are 4.05×10^{-4} and 3×10^{-3}, respectively. These values imply, for one thing, that the influence of using pseudo stochastic drag and lift coefficient in a wake oscillator model is limited. For another thing, it is found that the scatter in vibration prediction corresponding to the IL vibration is one order of magnitude larger than that in CF direction.

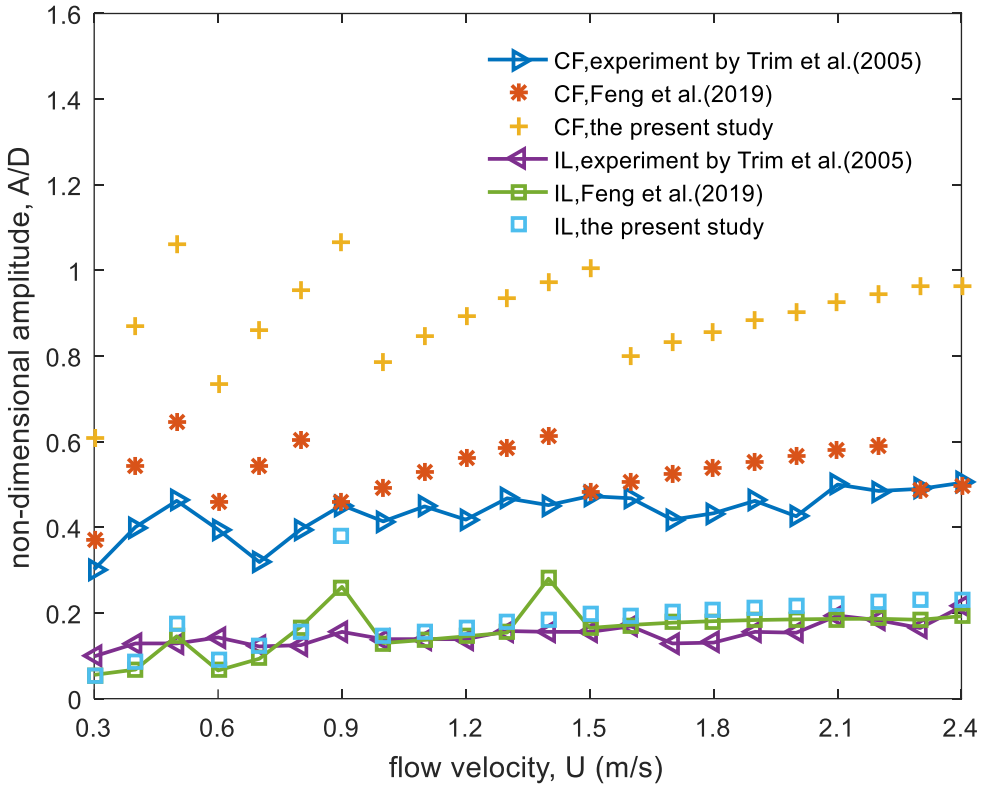

Figure 6 Numerical predicted spatial mean of temporal non-dimensional displacement standard deviation (STD/D) by wake oscillator model with and without considering random effect (Feng et al., 2019), compared to the experimental results (Trim et al., 2005).

Figure 6 depicts the variation of the averaged ξ, calculated by averaging 100 pseudo-stochastic model predictions of ξ, in both CF and IL directions with the flow velocity. In order to discern the influence of random drag and lift coefficients on the model prediction, the results by Feng et al. (2019) are included. It should be noted that both study of Feng et al. (2019) and the present study share the same model but have different sets of parameters. More specifically , while the model parameters in the study of Feng et al. (2019) are specified following the experiment (Trim et al., 2005), the stochastic model proposed in the present study specifies the parameters as pseudo stochastic variables whose statistics calculated from the measurements/simulations reported in the literature. It is shown from the figure that the vibrations in the CF direction predicted by the model considering random effects are higher than the conventional predictions by, on average, 67.71%. It is postulated that this overestimation is attributed to the difference in the lift coefficients contained in the models. While the mean of the lift coefficients (C_{L0}) in the model of the present study is 0.4121, the lift coefficient in the study of Feng et al. (2019) is 0.3. It should be addressed that the stochastic Cl model proposed in the present study is based on a large number of existing studies, in which the cylinder and flow under investigation are obviously different. For a specific case such as the one presented in the study, the model may not be the most appropriate choice. More specifically, the random variable models proposed in the present study could be erroneous for a specific case where the cylinder geometric characteristics and flow conditions are significantly different from the “averaged” situation derived from the existing literature reviewed in the present study. As regards the vibrations in the IL direction, both models with and without randomness are consistent in predicting vibration amplitudes. In addition, it is shown that the increases in C_{L0}, as 0.4121 in the present stochastic model comparing to 0.3 in the conventional model of Feng et al. (2019), has limited influences on the predictions of IL vibrations of the idealized cylinder. In fact, the predictions of IL vibrations made by the models with and without the random drag and lift coefficients differ, in most cases, within the range of 14.75% when the prediction made by the conventional model is used as the criterion. The noticeable exceptions, however, occur when the flow

velocities equals to 0.9m/s and 1.4m/s where the discrepancies reach 46.36% and 53.93% respectively. In a word, our model has some limitations at the current stage. The value of our study is not to propose a perfect model which is universally applicable to predict the vibration of cylinders in the flow under all conditions, but to shed lights into the stochastic effects and their modelling in the wake oscillator model. It is suggested that the stochastic model applicable for a specific case should be revised based on our findings and more relevant experimental data accumulating in the past or from independent numerical simulations, not from the broadly reviewed literature.

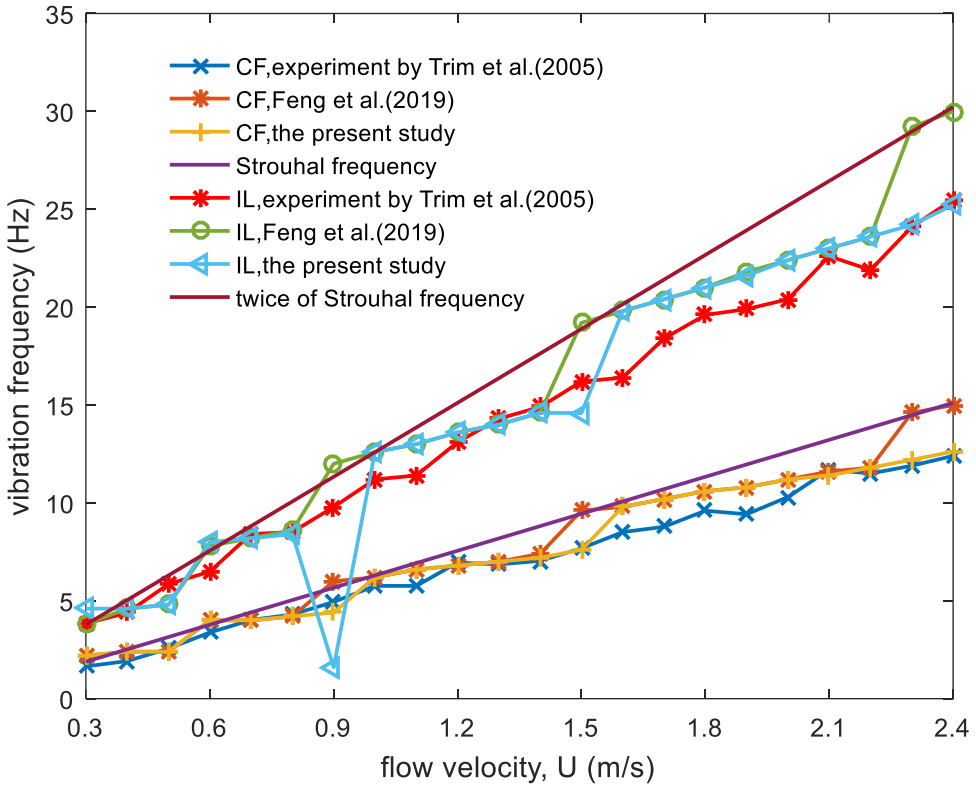

Figure 7 Numerical predicted vibration dominant frequency versus flow velocity by wake oscillator model with and without random effect, compared to the experimental results (Trim et al., 2005).

Figure 7 gives the variation of the dominant vibration frequency, which corresponds to the highest energy peak in the frequency spectrum of vibrations, with the flow velocity in both CF and IL directions. The two straight lines, shown as the references, represent the predictions made according to the Strouhal law of frequencies. In fact, the reference vibration frequency is assumed twice in the IL direction as in the CF direction following the observations in the studies of Blevins and Coughran (2009); Chaplin et al. (2005); Liu et al. (2014); Song et al. (2011); Trim et al. (2005). For the vibrations in the CF direction, when the flow velocity reaches 0.9m/s, 1.5m/s, 2.3m/s and 2.4m/s, the figure indicates that the conventional model without randomness obviously overestimates the vibration frequency. In fact, when the randomness is taken into consideration, the differences between predictions and the experimental measurements are reduced from 22.44% to 3.09%. The possible reason is that the random effect breaks the limitations in the vibration frequencies predicted by the deterministic model, and introduces vibrations at other frequencies, which is a better representation of the physical reality. As for the IL direction, the frequencies predicted from the model considering random effects are, at the above-mentioned four flow velocities, smaller than that from the model without randomness. Especially for the case where flow velocity equals 0.9 m/s, a very low frequency of 1.6 Hz dominates the vibration. The introduced chaos is more obvious and has a greater impact at this flow velocity. The reasonable guess may be

that complex interactions of the coupling system are motivated.

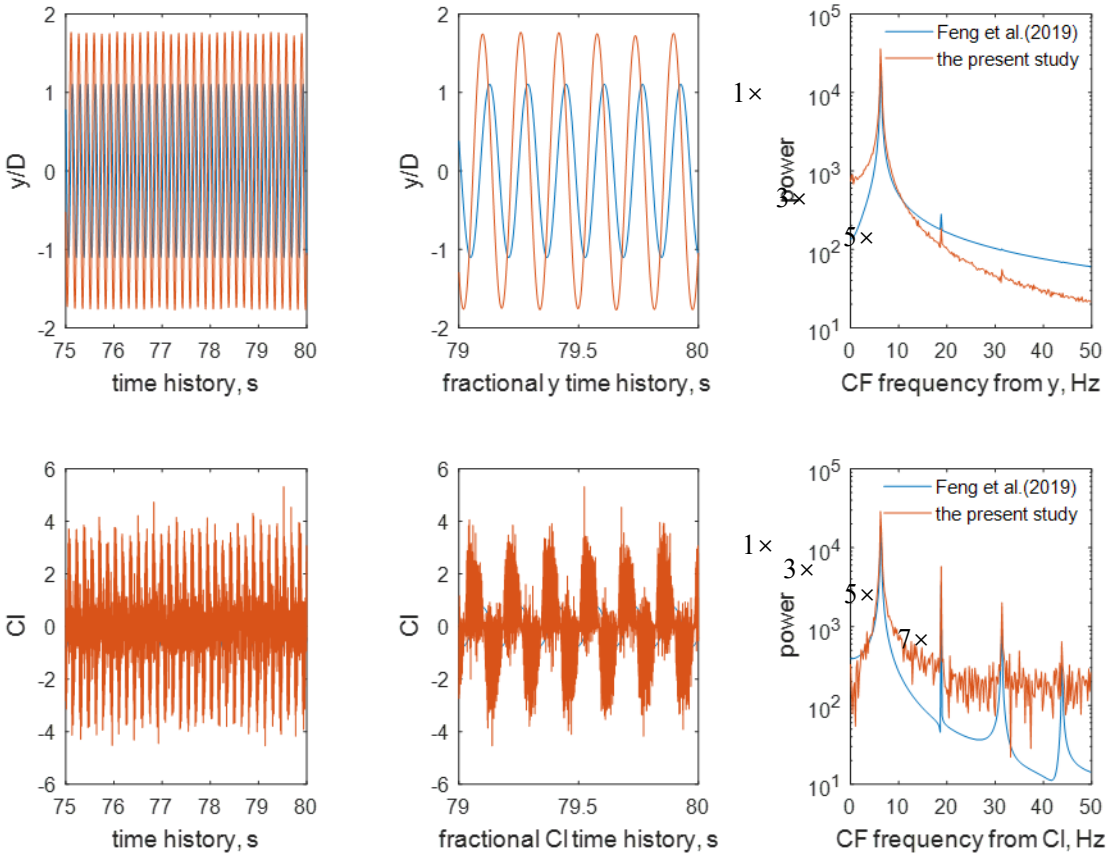

Figure 8 Spectral analysis of CF vibration frequency at the velocity of 1m/s predicted by wake oscillator model with and without random effect. The analysis is based on the time history extracted from *y* displacement (left) and lift coefficient (right), respectively.

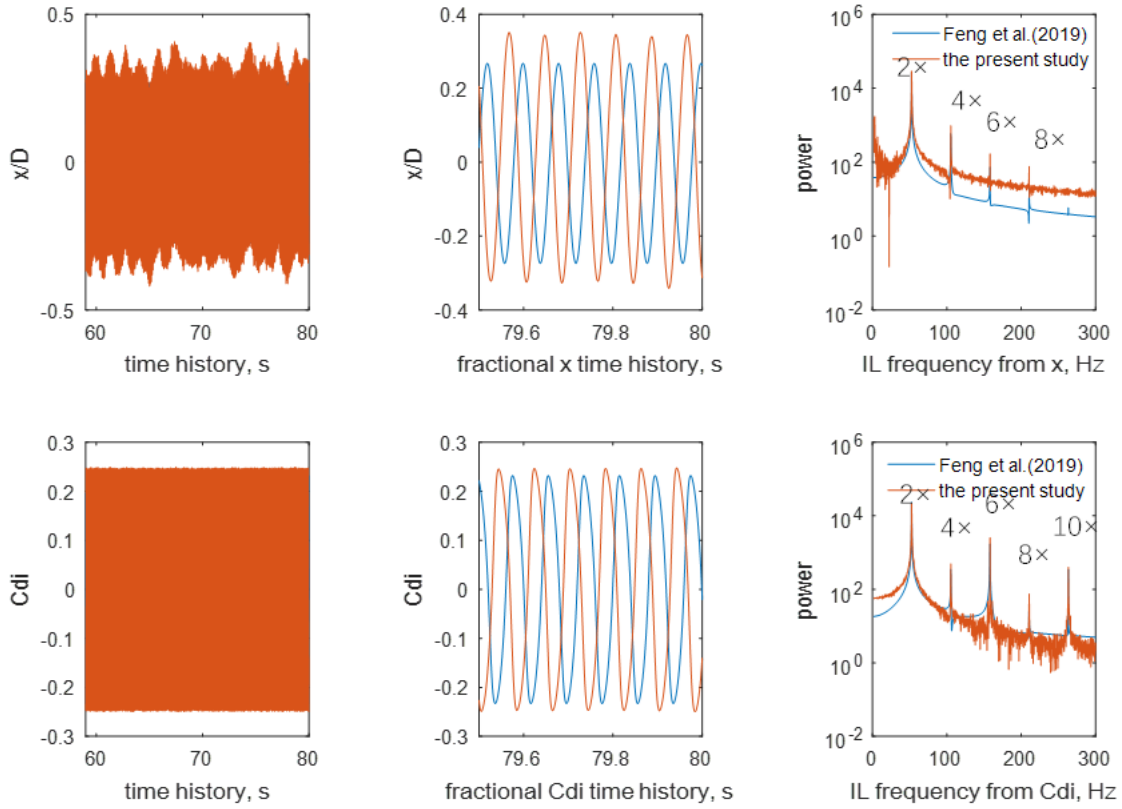

Figure 9 Spectral analysis of IL vibration frequency at the velocity of 1m/s predicted by wake oscillator model with and without random effect. The analysis is based on the time history extracted from *x* displacement (left) and drag coefficient (right), respectively.

Figures 8-11 give the time history of *x*/*y*/*Cdi*/*Cl* and their corresponding spectral analysis in both CF and IL directions at the velocities of 1m/s and 0.9m/s. The reason to present the figures at these two particular velocities is that they correspond to small and large discrepancies between model predictions with and without pseudo-stochastic parameterizations as indicated by Figures 6 and 7. These time histories given in the first column are extracted from t=55s/75s to t=80s when the simulations are stable. In order to illustrate the differences in the time history predictions, the second column show a fraction of the time history form the simulation, and the third column gives the spectra of the vibrations. Findings made from examining the figures are listed as follows,

(a) the amplitudes of vibrations are generally bigger from the model results with randomness. For the CF vibration, it is suggested to be attributed to the bigger lift coefficient. As for the vibrations in the IL direction, it is postulated that the vibrations in the CF direction, with larger amplitudes, transmits to the IL direction due to the complex interaction mechanism of the system. The overestimation of the amplitude is conservative for the prediction of structural vibrations.

(b) the pseudo-stochastic parameterizations of the drag and lift coefficient indeed induce additional frequency components in the vibrations of the cylinder in addition to a few major frequency peaks. In fact, the model with pseudo-stochastic parameterizations predicts a broadband stochastic process, which is more stand out for the large discrepancy case (Figures 10-11). Similar spectra are reported in the Norwegian Deepwater Program (NDP) dataset 2110 (Mukundan et al., 2009) and by Imaoka et al. (2015). NDP is an industrial project, in which a series of experiments were conducted to discern high mode VIV responses of long risers (Kaasen et al., 2000; Trim et al., 2005). In the model simulations conducted by Imaoka et al. (2015), vibration spectra from their normally-distributed random model and chaos model also imply broadband stochastic process with

several main frequency peaks. In contrast, the predictions from Faccinetti's model (Facchinetti et al., 2004) without randomness indicate that the VIV is a narrowband process. Therefore, it is found that the randomness is a significant factor for realistically reproducing the spectra of VIV for the long flexible cylinder.

(c) unexpected spectral peaks are surprisingly obtained from different time series (x displacement / drag coefficient and y displacement / lift coefficient). Frequency multiplication effect observed from a series of VIV experiments has been broadly reported in the literature (Gao et al., 2015a; Gao et al., 2015b; Kang and Jia, 2013; Kang et al., 2016; Liu et al., 2014; Song et al., 2011). In fact, it is found that the strains and displacements are usually oscillate at the frequency of f_o, $3\times f_o$, $5\times f_o$, etc in the CF direction and $2\times f_o$, $4\times f_o$, $6\times f_o$, etc in the IL direction as reported in many experimental studies (Gao et al., 2015a; Gao et al., 2015b; Song et al., 2016). Based on such observations, drag force and lift forces could be modelled as the summation of force fluctuations with specific frequencies as, $C_L = \sum_{k=1}^{\infty} C_{L0} sin[2\pi(2k-1)f_o t + \varphi_0]$ and $C_D = C_{D0} + \sum_{k=1}^{\infty} C_{Di0} sin[2\pi(2k)f_o t + \phi_0]$ (Wang et al., 2003). Tsatsos (2006) studied theoretical and numerical solution of the Van der Pol equation and decomposed a time series of the solution into time series with several specific frequencies. He gave an example ($\ddot{x} + x + a(x^2 - 1)\dot{x} = b\cos\omega t, a = 5, b = 40, \omega = 7$) where the Fourier spectrum consists a primary peak corresponding to one fundamental frequency and a series of secondary peaks whose frequencies are calculated by multiplying the fundamental frequency by integers. In another example ($a = 3, b = 5, \omega = 1.788$), the spectrum is continuous which means massive frequencies are involved and the signal shows the chaotic characteristic. To the best of authors' knowledge, this phenomenon has not been reported in the previous studies using the wake oscillator model. In Figures 8-11, the spectral peaks are marked as $1\times$, $3\times$, $5\times$…(CF direction) and $2\times$, $4\times$, $6\times$…(IL direction). It is shown in the figure that the frequency multiplication effect is well identified. Such findings imply that the wake oscillator model is capable of predicting the well-known frequency multiplication effect observed in the VIV of slender cylinders. When combing with the randomly drawn drag and lift coefficients, the spectra with clearly defined peaks and broad strips are also well reproduced.

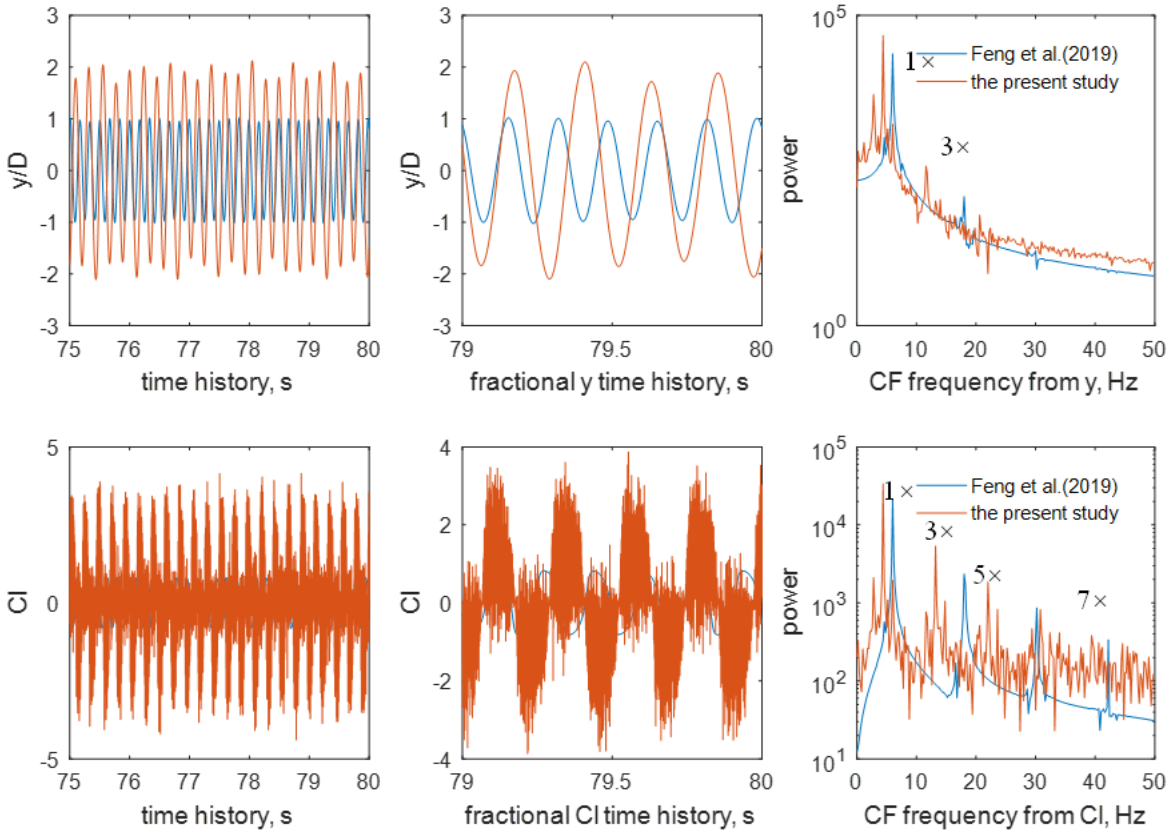

Figure 10 Spectral analysis of CF vibration frequency at the velocity of 0.9m/s predicted by wake oscillator model with and without random effect. The analysis is based on the time history extracted from *y* displacement (left) and lift coefficient (right), respectively.

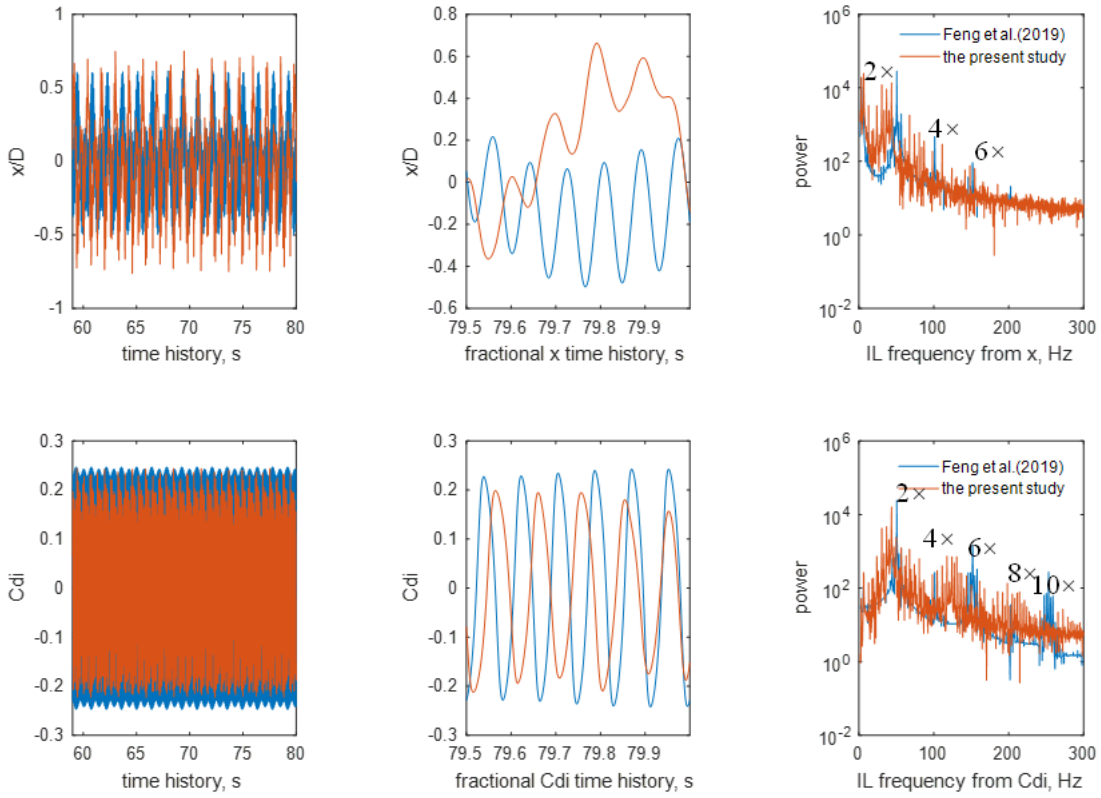

Figure 11 Spectral analysis of IL vibration frequency at the velocity of 0.9m/s predicted by wake oscillator model with and without random effect. The analysis is based on the time history extracted from *x* displacement (left) and drag coefficient (right), respectively.

4. Summary

A Euler-Bernoulli beam is coupled with the wake oscillator model with pseudo-stochastic drag and lift coefficients are used to predict the VIV of a long slender cylinder in both the IL and CF directions. In order to generate appropriate pseudo-stochastic lift and drag coefficient, the experimental measurements and numerical simulation results reported in the literature are referenced, and their statistics are calculated. Given the pseudo stochastic drag and lift coefficients whose statistics agreeing with the data extracted from the literature, structural motion equation is coupled with the Van der Pol's wake oscillator to predict the VIV of a long flexible cylinder identical to the model used by Trim et al. (2005) in their experiment. In the model, the tension is taken as a function of flow velocity. In order to discuss the influences of random drag and lift coefficients, the measurements taken by Trim et al. (2005) and the results from the study of Feng et al. (2019) are compared to the predictions made by the pseudo stochastic model.

It is found, from comparisons, that

(a) the inclusion of stochastic drag and lift coefficient has limited impacts on the prediction of the vibration amplitudes, and the influence on the IL vibration is more significant than the prediction concerning the CF vibrations;

(b) the vibration amplitudes predicted by the pseudo stochastic model are generally bigger than from the conventional model;

(c) the VIV of a long flexible cylinder, predicted by the pseudo stochastic model, are broadband stochastic process as revealed by the experiments of Mukundan et al. (2009);

(d) frequency multiplication effects observed in a series of experiments are realistically reproduced by both the stochastic and deterministic wake oscillator model.

The findings indicate the feasibility of including stochastic parameterizations into the wake oscillator model for the VIV analysis. It should be noted that the reliability and accuracy of the predictions depend on, to a large extent, the reliability and accuracy of the stochastic parameterization. In the prediction of VIV in a target case with specific configuration, it is suggested that a designated stochastic model specifically improved from the proposition of the present study should be employed.

Declarations of interest: none.

Acknowledgements

The authors would like to express their gratitude towards following organizations for financially supporting the work described in the present paper, which includes Shenzhen Science and Technology innovation Commission (Project No. WDZC20200819174646001). The numerical simulations are partially performed on Hefei advanced computing cente, to whom the authors would like to express their gratitude.

References

Achenbach, E., Heinecke, E., 1981. On vortex shedding from smooth and rough cylinders in the range of Reynolds numbers 6×10^3 to 5×10^6. Journal of Fluid Mechanics 109 (Journal of Fluid Mechanics), 239-251.

Agbaglah, G., Mavriplis, C., 2019. Three-dimensional wakes behind cylinders of square and circular cross-section: early and long-time dynamics. Journal of Fluid Mechanics 870, 419-432.

Allen, D.W., Henning, D.L., 2001. Surface Roughness Effects on Vortex-Induced Vibration of Cylindrical Structures at Critical and Supercritical Reynolds Numbers, Offshore Technology Conference, Houston, Texas.

Baarholm, G.S., Larsen, C.M., Lie, H., 2006. On fatigue damage accumulation from in-line and cross-flow vortex-induced vibrations on risers. Journal of Fluids & Structures 22 (1), 109-127.

Baranyi, L., Lewis, R.I., 2006. Comparison of a grid-based CFD method and vortex dynamics predictions of low Reynolds number cylinder flows. Aeronautical Journal, 63-71.

Bearman, P.W., 1969. On vortex shedding from a circular cylinder in the critical Reynolds number regime. Journal of Fluid Mechanics 37, 577-585.

Beaudan, P., Moin, P., 1994. Numerical experiments on the flow past a circular cylinder at sub-critical Reynolds number.

Belov, A., Martinelli, L., Jameson, A., 1995. A new implicit algorithm with multigrid for unsteady incompressible flow calculations.

Billah, K.Y.R., Shinozuka, M., 1991. Fluctuations of dynamic pressure and white noise assumption in flow-induced vibration problems. Journal of Sound and Vibration 147 (1), 179-183.

Blackburn, H.M., Melbourne, W.H., 1996. The effect of free-stream turbulence on sectional lift forces on a circular cylinder. Journal of Fluid Mechanics 306, 267-292.

Blevins, R.D., Coughran, C.S., 2009. Experimental Investigation of Vortex-Induced Vibration in One and Two Dimensions With Variable Mass, Damping, and Reynolds Number. Journal of Fluids Engineering 131 (10), 101202.

Bourdier, S., Chaplin, J.R., 2012. Vortex-induced vibrations of a rigid cylinder on elastic supports with end-stops, Part 1: Experimental results. Journal of Fluids & Structures 29, 62-78.

Braza, M., Chassaing, P., Ha Minh, H., 1985. A numerical study of the dynamics of different scale structures in the near wake of a circular cylinder in laminar to turbulent transition.

Braza, M., Chassaing, P., Ha Minh, H., 1986. Numerical study and physical analysis of the pressure and velocity fields in the near wake of a circular cylinder Journal of Fluid Mechanics 165, 79-130.

Breuer, M., 2000. A challenging test case for large eddy simulation: high Reynolds number circular cylinder flow. International Journal of Heat and Fluid Flow 21, 648-654.

Calhoun, D., 2002. A Cartesian Grid Method for Solving the Two-Dimensional Streamfunction-Vorticity Equations in Irregular Regions. Journal of Computational Physics 176, 231-275.

Cantwell, B., Coles, D., 1983. An experimental study of entrainment and transport in the turbulent near wake of a circular cylinder. Physics of Fluids 136 (8), 321-374.

Canuto, D., Taira, K., 2015. Two-dimensional compressible viscous flow around a circular cylinder. Journal of Fluid Mechanics 785, 349-371.

Cao, S., Huang, W., Gu, E., 2015. Vortex-induced vibration of an elastic cylinder considering fluid-structure interaction. Journal of Vibration and Shock 34 (1), 58-62.

Cavalcante, C.C.P., Bordalo, S.N., Morooka, C.K., Matt, C.G.C., Franciss, R., 2007. Experimental investigation on a laboratory-scale model of the fluid-pipe interaction on catenary risers for offshore petroleum production. Brazilian Journal of Petroleum and Gas 1 (2), 78-87.

Chaplin, J.R., Bearman, P.W., Huarte, F.J.H., Pattenden, R.J., 2005. Laboratory measurements of vortex-induced vibrations of a vertical tension riser in a stepped current. Journal of Fluids & Structures 21 (1), 3-24.

Chen, W., Li, X., Zhang, W., 2019. Shape optimization to suppress the lift oscillation of flow past a stationary circular cylinder. Physics of Fluids 31 (6).

Choi, J.-I., Oberoi, R.C., Edwards, J.R., Rosati, J.A., 2007. An immersed boundary method for complex incompressible flows. Journal of Computational Physics 224 (2), 757-784.

Dennis, S.C.R., Chang, G.Z., 1970. Numerical solutions for steady flow past a circular cylinder at Reynolds numbers up to 100 Journal of Fluid Mechanics 42, 471-489.

Derakhshandeh, J.F., Alam, M.M., 2019. A review of bluff body wakes. Ocean Engineering 182, 475-488.

Ding, H., Shu, C., Yeo, K.S., Xu, D., 2007. Numerical simulation of flows around two circular cylinders by mesh-free least square-based finite difference methods. International Journal for Numerical Methods in Fluids 53 (2), 305-332.

Dong, B., Li, W., Feng, Y., Sun, T., 2014. Lattice boltzmann simulation of a power-lawfluid past a circular cylinder. Chinese

Journal of Theoretical and Applied Mechanics 46 (1), 44-53.

Facchinetti, M.L., de Langre, E., Biolley, F., 2004. Coupling of structure and wake oscillators in vortex-induced vibrations. Journal of Fluids and Structures 19 (2), 123-140.

Farell, C., Blessmann, J., 1983. On critical flow around smooth circular cylinders. Journal of Fluid Mechanics 136, 375-391.

Feng, Y.L., S.W., L., Chen, D.Y., 2019. Predictions for combined In-Line and Cross-Flow VIV responses with a novel model for estimation of tension. Ocean Engineering 191 (1).

Fornberg, B., 1980. A numerical study of steady viscous flow past a circular cylinder Journal of Fluid Mechanics 98, 819-855.

Güven, O., Farell, C., Patel, V.C., 1980. Surface-roughness effects on the mean flow past circular cylinders. Journal of Fluid Mechanics 98 (4), 673-701.

Gao, Y., Fu, S., Cao, J., Chen, Y., 2015a. Experimental study on response performance of VIV of a flexible riser with helical strakes. Chinese Ocean Engineering Society 29 (5), 673-690.

Gao, Y., Fu, S., Wang, J., Song, L., Chen, Y., 2015b. Experimental study of the effects of surface roughness on the vortex-induced vibration response of a flexible cylinder. Ocean Engineering 103, 40-54.

Gartshore, I.S., 1984. Some effects of upstream turbulence on the unsteady lift forces imposed on prismatic two dimensional bodies. Transactions of the ASME. Journal of Fluids Engineering 106 (4), 418-424.

Gopalkrishnan, R., 1993. Vortex-induced forces on oscillating bluff cylinders, Massachusetts Institute of Technology.

Gresho, P.M., Chan, S.T., Lee, R.L., Upson, C.D., 1984. A modified finite element method for solving the time-dependent, incompressible Navier-Stokes equations. Part 2: Applications. International Journal for Numerical Methods in Fluids 4 (7), 619-640.

Gu, J.-j., An, C., Levi, C., Su, J., 2012. Prediction of vortex-induced vibration of long flexible cylinders modeled by a coupled nonlinear oscillator: Integral transform solution. Journal of Hydrodynamics, Ser. B 24 (6), 888-898.

Gu, J., Wang, Y., Zhang, Y., Duan, M., Levi, C., 2013. Analytical solution of mean top tension of long flexible riser in modeling vortex-induced vibrations. Applied Ocean Research 2013 (41), 1-8.

Gushchin, V.A., Shchennikov, V.V., 1974. A numerical method of solving the navier-stokes equations. 14 (2), 242-250.

He, X.Y., Doolen, G., 1997. Lattice Boltzmann method on curvilinear coordinates system: flow around a circular cylinder. Journal of Computational Physics 134 (2), 306-315.

Henderson, R.D., 1995. Details of the drag curve near the onset of vortex shedding. Physics of Fluids 7 (9), 2102-2104.

Hong, K.S., Shah, U.H., 2018. Vortex-induced vibrations and control of marine risers: A review. Ocean Engineering 152, 300-315.

Imaoka, K., Kobayashi, Y., Emaru, T., Hoshino, Y., 2014. Effect of the random component in the vortex-induced vibration, SICE Annual Conference (SICE) 2014, Hokkaido University, Sapporo, Japan.

Imaoka, K., Kobayashi, Y., Emaru, T., Hoshino, Y., 2015. Vortex-Induced Vibration of an Elastically-Supported Cylinder Considering Random Flow Effects. Sice Jcmsi 8 (2), 131-138.

Jiang, M., Liu, Z., 2019. A boundary thickening-based direct forcing immersed boundary method for fully resolved simulation

of particle-laden flows. Journal of Computational Physics 390, 203-231.

Jordan, S.K., Fromm, J.E., 1972. Oscillatory drag, lift, and torque on a circular cylinder in a uniform flow. Physics of Fluids 15 (3), 371-376.

Kaasen, K.E., Lie, H., Solaas, F., Vandiver, J.K., 2000. Norwegian Deepwater Program: Analysis of Vortex-Induced Vibrations of Marine Risers Based on Full-Scale Measurements, Offshore Technology Conference, Houston, Texas.

Kang, S., 2003. Characteristics of flow over two circular cylinders in a side-by-side arrangement at low Reynolds numbers. Physics of Fluids 15 (9), 2486-2498.

Kang, S.K., Hassan, Y.A., 2011. A comparative study of direct-forcing immersed boundary-lattice Boltzmann methods for stationary complex boundaries. International Journal for Numerical Methods in Fluids 66 (9), 1132-1158.

Kang, Z., Jia, L., 2013. An experiment study of a cylinder's two degree of freedom VIV trajectories. Ocean Engineering 70, 129-140.

Kang, Z., Ni, W., Sun, L., 2016. An experimental investigation of two-degrees-of-freedom VIV trajectories of a cylinder at different scales and natural frequency ratios. Ocean Engineering 126, 187-202.

Karagiozis, K., Kamakoti, R., Pantano, C., 2010. A low numerical dissipation immersed interface method for the compressible Navier-Stokes equations. Journal of Computational Physics 229 (3), 701-727.

Khalak, A., Williamson, C.H.K., 1999. Motions, forces and mode transitions in vortex-induced vibrations at low mass-damping. Journal of Fluids and Structures 13 (7-8), 813-851.

Kim, J., Kim, D., Choi, H., 2001. An immersed-boundary finite-volume method for simulations of flow in complex geometries. Journal of Computational Physics 171 (1), 132-150.

Konstantinidis, E., Bouris, D., 2017. Drag and inertia coefficients for a circular cylinder in steady plus low-amplitude oscillatory flows. Applied Ocean Research 65, 219-228.

Lai, M.C., Peskin, C.S., 2000. An immersed boundary method with formal second-order accuracy and reduced numerical viscosity. Journal of Computational Physics 160 (2), 705-719.

Lausova, L., Kolos, I., Michalcova, V., 2019. Comparison of 2D grid simulations for flow past cylinder at high Reynolds numbers. Civil and Environmental Engineering 15 (1), 70-78.

Le, D.V., Khoo, B.C., Lim, K.M., 2008. An implicit-forcing immersed boundary method for simulating viscous flows in irregular domains. Computer Methods in Applied Mechanics and Engineering 197 (25-28), 2119-2130.

Lecointe, Y., Piquet, J., 1984. On the use of several compact methods for the study of unsteady incompressible viscous-flow round a circular-cylinder. Computers & Fluids 12 (4), 255-280.

Lecointe, Y., Piquet, J., 1989. Flow structure in the wake of an oscillating cylinder. Journal of Fluids Engineering-Transactions of the Asme 111 (2), 139-148.

Lee, L., Allen, D., 2010. Vibration frequency and lock-in bandwidth of tensioned, flexible cylinders experiencing vortex shedding. Journal of Fluids and Structures 26 (4), 602-610.

Leehey, P., Hanson, C.E., 1971. Aeolian tones associated with resonant vibration. Journal of Sound and Vibration 13 (4), 465-483.

Lie, H., Kaasen, K.E., 2006. Modal analysis of measurements from a large-scale VIV model test of a riser in linearly sheared flow. Journal of Fluids & Structures 22 (4), 557-575.

Linnick, M.N., Fasel, H.F., 2005. A high-order immersed interface method for simulating unsteady incompressible flows on irregular domains. Journal of Computational Physics 204 (1), 157-192.

Liu, C., Gao, Y.-y., Qu, X.-c., Wang, B., Zhang, B.-f., 2019a. Numerical Simulation on Flow Past Two Side-by-Side Inclined Circular Cylinders at Low Reynolds Number. China Ocean Engineering 33 (3), 344-355.

Liu, C., Hu, C., 2018. An adaptive multi-moment FVM approach for incompressible flows. Journal of Computational Physics 359, 239-262.

Liu, C., Zheng, X., Sung, C.H., 1998. Preconditioned multigrid methods for unsteady incompressible flows. Journal of Computational Physics 139 (1), 35-57.

Liu, M., Li, S.Y., Li, H.X., Li, S.K., Chen, Z.Q., 2019b. Reynolds number effects on wind-induced responses of a 243-m-high solar tower in elastic wind tunnel tests. Journal of Aerospace Engineering 32 (4).

Liu, Q., Mao, L., Zhou, S., 2014. Experimental study of the effect of drilling pipe on vortex-induced vibration of drilling risers. Journal of Vibroengineering 16 (4), 1842-1853.

Liu, X., Thompson, D.J., Hue, Z., 2019c. Numerical investigation of aerodynamic noise generated by circular cylinders in cross-flow at Reynolds numbers in the upper subcritical and critical regimes. International Journal of Aeroacoustics 18 (4-5), 470-495.

Lucor, D., Karniadakis, G.E., 2004. Predictability and uncertainty in flow–structure interactions. European Journal of Mechanics, B/Fluids 23 (1), 41-49.

Marx, Y.P., 1994. Time integration schemes for the unsteady incompressible navier-stokes equations. Journal of Computational Physics 112 (1), 182-209.

Michalcova, V., Kolos, I., Lausova, L., 2019. Numerical modeling of the aerodynamic coefficient of the circular cylinder. AIP Conference Proceedings 2116.

Mirzaee, H., Rafee, R., Ahmadi, G., 2019. Inertial impaction of particles on a circular cylinder for a wide range of Reynolds and P numbers: a comparative study. Journal of Aerosol Science 135, 86-102.

Mukundan, H., Modarres-Sadeghi, Y., Dahl, J.M., Hover, F.S., Triantafyllou, M.S., 2009. Monitoring VIV fatigue damage on marine risers. Journal of Fluids & Structures 25 (4), 617-628.

Nieuwstadt, F., Keller, H.B., 1973. Viscous flow past circular cylinders. Computers & Fluids 1 (1), 59-71.

Norberg, C., 1993. Pressure Forces on a Circular Cylinder in Cross Flow, IUTAM Symposium. Springer-Verlag.

Palkin, E., Hadziabdic, M., Mullyadzhanov, R., Hanjalic, K., 2018. Control of flow around a cylinder by rotary oscillations at a high subcritical Reynolds number. Journal of Fluid Mechanics 855, 236-266.

Pan, Z.Y., Cui, W.C., Miao, Q.M., 2007. Numerical simulation of vortex-induced vibration of a circular cylinder at low mass-damping using RANS code. Journal of Fluids and Structures 23 (1), 23-37.

Park, H., Pan, X., Lee, C., Choi, J.-I., 2016. A pre-conditioned implicit direct forcing based immersed boundary method for incompressible viscous flows. Journal of Computational Physics 314, 774-799.

Park, J., Kwon, K., Choi, H., 1998. Numerical solutions of flow past a circular cylinder at Reynolds numbers up to 160. Ksme International Journal 12 (6), 1200-1205.

Qu, L., Norberg, C., Davidson, L., Peng, S.-H., Wang, F., 2013. Quantitative numerical analysis of flow past a circular cylinder at Reynolds number between 50 and 200. Journal of Fluids and Structures 39, 347-370.

Rahman, M.M., Karim, M.M., Alim, M.A., 2007. Numerical investigation of unsteady flow past a circular cylinder using 2-d finite volume method. Journal of Naval Architecture and Marine Engineering (4), 27-42.

Rogers, S.E., Kwak, D., 1990. Upwind differencing scheme for the time-accurate incompressible navier-stokes equations. Aiaa Journal 28 (2), 253-262.

Rosenfeld, M., Kwak, D., Vinokur, M., 1991. A fractional step solution method for the unsteady incompressible navier-stokes equations in generalized coordinate systems. Journal of Computational Physics 94 (1), 102-137.

Roshko, A., 1961. Experiments on the flow past a circular cylinder at very high Reynolds number. Journal of Fluid Mechanics 10 (3), 345-356.

Russell, D., Wang, Z.J., 2003. A cartesian grid method for modeling multiple moving objects in 2D incompressible viscous flow. Journal of Computational Physics 191 (1), 177-205.

Saiki, E.M., Biringen, S., 1996. Numerical simulation of a cylinder in uniform flow: Application of a virtual boundary method. Journal of Computational Physics 123 (2), 450-465.

Schewe, G., 1983. On the force fluctuations acting on a circular cylinder in crossflow from subcritical up to transcritical Reynolds number. Journal of Fluid Mechanics 133, 265-285.

Shih, W.C.L., Wang, C., Coles, D., Roshko, A., 1993. Experiments on flow past rough circular cylinders at large Reynolds numbers. Journal of Wind Engineering and Industrial Aerodynamics 49 (1), 351-368.

Shoshani, O., 2018. Deterministic and stochastic analyses of the lock-in phenomenon in vortex-induced vibrations. Journal of Sound and Vibration 434, 17-27.

Singh, S.P., Mittal, S., 2005. Flow past a cylinder: shear layer instability and drag crisis. International Journal for Numerical Methods in Fluids 47 (1), 75-98.

Song, J.-n., Lu, L., Teng, B., Park, H.-i., Tang, G.-q., Wu, H., 2011. Laboratory tests of vortex-induced vibrations of a long flexible riser pipe subjected to uniform flow. Ocean Engineering 38 (11-12), 1308-1322.

Song, L., Fu, S., Zeng, Y., Chen, Y., 2016. Hydrodynamic Forces and Coefficients on Flexible Risers Undergoing Vortex-Induced Vibrations in Uniform Flow. Journal of Waterway, Port, Coastal, and Ocean Engineering 142 (4), 04016001.

Srinil, N., Opinel, P.-A., Tagliaferri, F., 2018. Empirical sensitivity of two-dimensional nonlinear wake–cylinder oscillators in cross-flow/in-line vortex-induced vibrations. Journal of Fluids and Structures 83, 310-338.

Szepessy, S., Bearman, P.W., 1992. Aspect ratio and end plate effects on vortex shedding from a circular cylinder. Journal of Fluid Mechanics 234, 191-217.

Taira, K., Colonius, T., 2007. The immersed boundary method: A projection approach. Journal of Computational Physics 225 (2), 2118-2137.

Takami, H., Keller, H.B., 1969. Steady two-dimensional viscous flow of an incompressible fluid past a circular cylinder. Physics

of Fluids, II 51-56.

Thakur, A., Liu, X., Marshall, J.S., 2004. Wake flow of single and multiple yawed cylinders. Journal of Fluids Engineering-Transactions of the Asme 126 (5), 861-870.

Travin, A., Shur, M., Strelets, M., Spalart, P., 2000. Detached-eddy simulations past a circular cylinder. Flow Turbulence and Combustion 63 (1-4), 293-313.

Trim, A.D., Braaten, H., Lie, H., Tognarelli, M.A., 2005. Experimental investigation of vortex-induced vibration of long marine risers. Journal of Fluids and Structures 21 (3), 335-361.

Tritton, D.J., 1959. Experiments on the flow past a circular cylinder at low Reynolds numbers. Journal of Fluid Mechanics 6 (4), 547-567.

Tsatsos, M., 2006. Theoretical and numerical study of the Van der Pol equation, School of Sciences, Department of Physics. Aristotle University of Thessaloniki

Tuann, S.Y., Olson, M.D., 1978. Numerical studies of flow around a circular-cylinder by a finite-element method. Computers & Fluids 6 (4), 219-240.

Wang, X.Q., So, R.M.C., Chan, K.T., 2003. A non-linear fluid force model for vortex-induced vibration of an elastic cylinder. Journal of Sound and Vibration 260 (2003), 287-305.

Wei, Z.L., Sun, D.J., Yin, X.Y., 2006. A numerical simulation of flow around a transversely oscillating hydrofoil in the wake of a circular cylinder. Journal of Hydrodynamics 21 (3), 299-308.

West, G.S., Apelt, C.J., 1993. Measurements of fluctuating pressures and forces on a circular-cylinder in the reynolds-number range 10^4 to 2.5 x 10^5. Journal of Fluids and Structures 7 (3), 227-244.

Wright, J.A., Smith, R.W., 2001. An edge-based method for the incompressible Navier-Stokes equations on polygonal meshes. Journal of Computational Physics 169 (1), 24-43.

Wu, J., Shu, C., 2009. Implicit velocity correction-based immersed boundary-lattice Boltzmann method and its applications. Journal of Computational Physics 228 (6), 1963-1979.

Ye, T., Mittal, R., Udaykumar, H.S., Shyy, W., 1999. An accurate Cartesian grid method for viscous incompressible flows with complex immersed boundaries. Journal of Computational Physics 156 (2), 209-240.

Zdravkovich, M.M., 1997. Flow around circular cylinders. Oxford University Press.

Zhang, J.F., Dalton, C., 1997. Interaction of a steady approach flow and a circular cylinder undergoing forced oscillation. Journal of Fluids Engineering-Transactions of the Asme 119 (4), 808-813.

Zhou, C.Y., So, R.M.C., Lam, K., 1999. Vortex-induced vibrations of an elastic circular cylinder. Journal of Fluids and Structures 13 (2), 165-189.

Zhou, X., Dong, B., Chen, C., Li, W., 2019. A thermal LBM-LES model in body-fitted coordinates: Flow and heat transfer around a circular cylinder in a wide Reynolds number range. International Journal of Heat and Fluid Flow 77, 113-121.

Zong, Z., Feng, W.U., 2017. A Summary of the Pseudo-Excitation Method for VIV Fatigue Damage Analysis of Marine Risers. Applied Mathematics & Mechanics 38 (1), 60-66.

APPENDIX: LIST OF SYMBOLS

M the sum of structure mass m_s and added fluid mass per unit length

F hydrodynamic force per unit length, with components Fx and Fy

r the deflection, a vector, with components x and y

EI bending stiffness

E Young's modulus

T axial tension

C_a added mass coefficient

ρ density of seawater

D diameter of the riser

R damping coefficient due to hydrodynamic damping and structural damping

R_f damping coefficient due to hydrodynamic force

R_s damping coefficient due to structure force

γ parameter determined through experiments

Ω_f vortex shedding frequency

Ω_n natural frequency of the riser in air

Ω_s natural frequency of the riser in water

ξ_D damping ratio

T_{ini} tension force before deflection

A cross section area of the riser

L length of the riser

ΔL prolongation of the riser

F_x external force exerted perpendicularly on the model in the x direction

F_y external force exerted perpendicularly on the model in the y direction

f_D mean drag force per unit length

f_D' fluatuating drag force per unit length

f_L lift force per unit length

C_D mean drag coefficient of a stationary rigid cylinder

C_{D0} the amplitude of mean drag coefficient of a stationary rigid cylinder

$\overline{C_{D0}}$ mean of the mean drag coefficient of a stationary rigid cylinder for a certain flow regime

$\delta_{C_{D0}}$ standard deviation of the mean drag coefficient of a stationary rigid cylinder for a certain flow regime

$Y_{RMS/D}$ the amplitude of vibration in the CF direction

C_{Di} vortex shedding drag coefficient

C_{Di0} the amplitude of vortex shedding drag coefficient

C_{L0} lift coefficient of a stationary rigid cylinder

C_L lift coefficient varying with time

$\overline{C_{L0}}$ mean of the lift coefficient of a stationary rigid cylinder for a certain flow regime

$\delta_{C_{L0}}$ standard deviation of the lift coefficient of a stationary rigid cylinder for a certain flow regime

p in line wake variable

q cross flow wake variable

ε_x, ε_y, A_x, A_y non-dimensional parameters estimated through experiments

S_t Strouhal numbe

$\overline{C_{D0}}\delta_{C_{D0}}\overline{C_{L0}}\delta_{C_{L0}}$